

## Nanotechnology, smartness and orthotropic nonhomogeneous elastic medium effects on buckling of piezoelectric pipes

Farhad Mosharrafian and Reza Kolahchi\*

*Department of Civil Engineering, Khomein Branch, Islamic Azad University, Khomein, Iran*

*(Received December 3, 2015, Revised April 16, 2016, Accepted April 21, 2016)*

**Abstract.** The effects of nanotechnology and smartness on the buckling reduction of pipes are the main contributions of present work. For this ends, the pipe is simulated with classical piezoelectric polymeric cylindrical shell reinforced by armchair double walled boron nitride nanotubes (DWBNNs), The structure is subjected to combined electro-thermo-mechanical loads. The surrounding elastic foundation is modeled with a novel model namely as orthotropic nonhomogeneous Pasternak medium. Using representative volume element (RVE) based on micromechanical modeling, mechanical, electrical and thermal characteristics of the equivalent composite are determined. Employing nonlinear strains-displacements and stress-strain relations as well as the charge equation for coupling of electrical and mechanical fields, the governing equations are derived based on Hamilton's principal. Based on differential quadrature method (DQM), the buckling load of pipe is calculated. The influences of electrical and thermal loads, geometrical parameters of shell, elastic foundation, orientation angle and volume percent of DWBNNs in polymer are investigated on the buckling of pipe. Results showed that the generated  $\Phi$  improved sensor and actuator applications in several process industries, because it increases the stability of structure. Furthermore, using nanotechnology in reinforcing the pipe, the buckling load of structure increases.

**Keywords:** nanotechnology; smartness; pipe; piezoelectric; orthotropic nonhomogeneous Pasternak medium

### 1. Introduction

Composites offer advantageous characteristics of different materials with qualities that none of the constituents possess. Nanocomposites developed in recent years, have received much attention amongst researchers due to provision of new properties and exploiting unique synergism between materials. Polyvinylidene fluoride (PVDF) is an ideal piezoelectric matrix due to characteristics including flexibility in thermoplastic conversion techniques, excellent dimensional stability, abrasion and corrosion resistance, high strength and capability of maintaining its mechanical properties at elevated temperature. It has therefore found multiple applications in nanocomposites in a wide range of industries including oil and gas pipelines, petrochemical, wire and cable, electronics, automotive and construction. Boron nitride nanotubes (BNNTs) used as the matrix reinforcers, apart from having high mechanical, electrical and chemical properties, present more

---

\*Corresponding author, Ph.D., E-mail: [r.kolahchi@gmail.com](mailto:r.kolahchi@gmail.com)

resistant to oxidation than other conventional nano-reinforcers such as carbon nanotubes (CNTs), Hence, they are used for high temperature applications (MerhariHybrid 2002, Schwartz 2002, Yu *et al.* 2006, Vang 2006, Kotsilkova 2007, Brockmann 2009),

Elastic buckling of a thin cylindrical shell was studied by Karam *et al.* (1995), Agrawal and Sobel (1977) investigated the weight compressions of cylindrical shells with various stiffness under axial compression. Buckling of cylindrical shells with metal foam cores was presented by Hutchinson and He (2000), Elastic stability of cylindrical shell with an elastic core under axial compression was investigated by Ghorbanpour Arani *et al.* (2007) using energy method. Ye *et al.* (2011), however, investigated buckling of a thin-walled cylindrical shell with foam core under axial compression. Junger and Mass (1952) studied coupled vibrations of fluid-filled cylindrical shells based on shear shell theory and discussed the free vibration of orthotropic cylindrical shells filled partially or completely with an incompressible, non-viscous fluid. The static instability of a nanobeam with geometrical imperfections embedded in elastic foundation was investigated by Mohammadi *et al.* (2014), Using semi-analytical finite strip method, the buckling behavior of laminated composite deep as well as thick shells of revolution under follower forces which remain normal to the shell was investigated by Khayat *et al.* (2016),

With respect to developmental works on buckling of the cylindrical shells, it should be noted that none of the research mentioned above, have considered smart composites and their specific characteristics. Micromechanical modeling which has the potential to take into account the electrical load was used by Tan and Tong (2001) for studying an imperfect textile composite. However, neither the matrix nor the reinforced material used in the composite employed in this work was smart. Buckling of BNNTs reinforced piezoelectric polymeric composites subjected to combined electro-thermo-mechanical loadings were investigated by Salehi-Khojin and Jalili (2008), Ghorbanpour Arani *et al.* (2011a, 2011b) carried out a stress analysis in cylinder and spheres made from piezoelectric materials using analytical method and ANSYS software. Rahmani *et al.* (2010) investigated free vibration response of composite sandwich cylindrical shells with flexible core. Buckling and vibration analysis of plate/shell structures via a smoothed quadrilateral flat shell element with in-plane rotations were studied by Nguyen-Van (2011), Electro-thermo-mechanical nonlinear buckling of a piezoelectric polymeric cylindrical shell reinforced by DWBNNTs was studied by Mosallaie Barzoki *et al.* (2013), Ghorbanpour Arani *et al.* (2015) investigated nonlinear vibration and instability of a fluid conveying smart composite microtube based on the modified couple stress theory and Timoshenko beam model. Viscous fluid induced nonlinear free vibration and instability analysis of a functionally graded carbon nanotube-reinforced composite (CNTRC) cylindrical shell integrated with two uniformly distributed piezoelectric layers on the top and bottom surfaces of the cylindrical shell were presented by Rabani Bidgoli (2015), An accurate buckling analysis for piezoelectric fiber-reinforced composite (PFRC) cylindrical shells subjected to combined loads comprising compression, external voltage and thermal load was presented by Sun *et al.* (2016), Buckling response of piezoelectric cylindrical composite panels reinforced with carbon nano-tubes subjected to axial load was studied by Nasihatgozar *et al.* (2016),

None of the above mentioned works have not considered both nanotechnology and smartness effects on the buckling analysis of pipes. However, in the present work, nonlinear buckling of piezoelectric pipes embedded in an orthotropic nonhomogeneous Pasternak medium is studied considering nanotechnology and smartness effects. The pipe is reinforced with DWBNNTs and polarized in axial direction. The influences of electrical and thermal loads, geometrical parameters of shell, elastic foundation, orientation angle and volume percent of DWBNNTs in polymer on the

buckling of pipe are investigated.

## 2. Classical shell theory

Based on classical shell model, the displacement components of an arbitrary point anywhere are written as: (Brush and Almroth 1975)

$$\begin{aligned} U(x, \theta, z, t) &= u(x, \theta, t) - z \frac{\partial w(x, \theta, t)}{\partial x}, \\ V(x, \theta, z, t) &= v(x, \theta, t) - z \frac{\partial w(x, \theta, t)}{R \partial \theta}, \\ W(x, \theta, z, t) &= w(x, \theta, t), \end{aligned} \quad (1)$$

where,  $U, V, W$  are the displacements of a arbitrary point of the shell in the axial, circumferential and radial directions, respectively,  $u, v, w$  are the displacements of points on the middle surface of the shell and  $z$  is the distance of the arbitrary point of the shell from the middle surface. Substituting Eq. (1) into the total strain tensor (Brush and Almroth 1975), the mechanical and thermal strains may be written as follows

$$\varepsilon = \begin{Bmatrix} \varepsilon_{xx} \\ \varepsilon_{\theta\theta} \\ \varepsilon_{x\theta} \end{Bmatrix} + \begin{Bmatrix} -\alpha_x \Delta T \\ -\alpha_\theta \Delta T \\ 0 \end{Bmatrix}, \quad (2)$$

where  $(\alpha_x, \alpha_\theta)$  and  $\Delta T$  are thermal expansion and temperature gradient, respectively. The mechanical strain components  $\varepsilon_{xx}, \varepsilon_{\theta\theta}, \varepsilon_{x\theta}$  at an arbitrary point of the shell are related to the middle surface strains  $\varepsilon_{x,0}, \varepsilon_{\theta,0}, \varepsilon_{x\theta,0}$  and changes in the curvature and torsion of the middle surface  $k_x, k_\theta, k_{x\theta}$  as follows (Mosallaie Barzoki *et al.* 2013)

$$\begin{aligned} \begin{Bmatrix} \varepsilon_x \\ \varepsilon_\theta \\ \gamma_{x\theta} \end{Bmatrix}_{shell} &= \begin{Bmatrix} \varepsilon_{xm} \\ \varepsilon_{\theta m} \\ \gamma_{x\theta m} \end{Bmatrix}_L + \begin{Bmatrix} \varepsilon_{xm} \\ \varepsilon_{\theta m} \\ \gamma_{x\theta m} \end{Bmatrix}_{NL} - z \begin{Bmatrix} k_x \\ k_\theta \\ k_{x\theta} \end{Bmatrix} \\ &= \begin{Bmatrix} \frac{\partial u}{\partial x} \\ \frac{\partial v}{R \partial \theta} + \frac{w}{R} \\ \frac{\partial u}{R \partial \theta} + \frac{\partial v}{\partial x} \end{Bmatrix} + \begin{Bmatrix} \frac{1}{2} \left( \frac{\partial w}{\partial x} \right)^2 \\ \frac{1}{2} \left( \frac{\partial w}{R \partial \theta} \right)^2 \\ \frac{\partial w}{\partial x} \frac{\partial w}{R \partial \theta} \end{Bmatrix} - z \begin{Bmatrix} \frac{\partial^2 w}{\partial x^2} \\ \frac{\partial^2 w}{R^2 \partial \theta^2} \\ 2 \frac{\partial^2 w}{R \partial x \partial \theta} \end{Bmatrix}. \end{aligned} \quad (3)$$

## 3. Constitutive equations of piezoelectric materials

In a piezoelectric material, application of an electric field to it will cause a strain proportional to the mechanical field strength, and vice versa. The constitutive equations for stresses  $\sigma$  and strains  $\epsilon$  matrix on the mechanical side, as well as flux density  $D$  and field strength  $E$  matrix on the electrostatic side, may be arbitrarily combined as follows (Ghorbanpour Arani *et al.* 2015)

$$\sigma_i = C_{ij}(\epsilon_j - \alpha_{ci}\Delta T) - e_{ik}E_k, \tag{4}$$

$$D_m = e_{mj}(\epsilon_j - \alpha_{ci}\Delta T) + \epsilon_{mk}E_k, \tag{5}$$

where  $C_{ij}$ ,  $e_{ij}$  and  $\epsilon_{ii}$  ( $i,j=1,\dots,6$ ) are elastic, piezoelectric and dielectric constants, respectively. Also, the electric field may be written in term of electric potential as

$$E_k = -\nabla\phi. \tag{6}$$

The transformed elastic constants are defined as

$$[Q] = [R][C][R]^T, \tag{7}$$

where  $[R]$  is the transfer matrix which can be defined as

$$[R] = \begin{bmatrix} \cos^2(\theta) & \sin^2(\theta) & 0 & 0 & 0 & -\sin(2\theta) \\ \sin^2(\theta) & \cos^2(\theta) & 0 & 0 & 0 & \sin(2\theta) \\ 0 & 0 & 1 & 0 & 0 & 0 \\ 0 & 0 & 0 & \cos(\theta) & \sin(\theta) & 0 \\ 0 & 0 & 0 & -\sin(\theta) & \cos(\theta) & 0 \\ \sin(\theta)\cos(\theta) & -\sin(\theta)\cos(\theta) & 0 & 0 & 0 & \cos^2(\theta) - \sin^2(\theta) \end{bmatrix}. \tag{8}$$

here,  $\theta$  is the angle between the global and local cylindrical co-ordinates, which corresponds to the orientation angle between DWBNNTs and the main axis of the matrix.

Based on classical shell theory, the constitute equations of (4) and (5) may be simplified as

$$\begin{Bmatrix} \sigma_x \\ \sigma_\theta \\ \tau_{x\theta} \\ D_x \end{Bmatrix} = \begin{bmatrix} Q_{11} & Q_{12} & 0 & -e_{11} \\ Q_{12} & Q_{22} & 0 & -e_{12} \\ 0 & 0 & Q_{66} & 0 \\ e_{11} & e_{12} & 0 & \epsilon_{11} \end{bmatrix} \begin{Bmatrix} \epsilon_x - \alpha_x\Delta T \\ \epsilon_\theta - \alpha_\theta\Delta T \\ \gamma_{x\theta} \\ E_x \end{Bmatrix}, \tag{9}$$

Based on micro-mechanical model, the mechanical, thermal and electrical properties of the composite as shown in Eq. (9) are (Mosallaie Barzoki *et al.* 2013)

$$Q_{11} = \frac{C_{11}^r C_{11}^m}{\rho C_{11}^m + (1-\rho)C_{11}^r}, \tag{10}$$

$$Q_{12} = C_{11} \left[ \frac{\rho C_{12}^r}{C_{11}^r} + \frac{(1-\rho)C_{12}^m}{C_{11}^m} \right], \tag{11}$$

$$Q_{22} = \rho C_{22}^r + (1-\rho)C_{22}^m + \frac{C_{12}^2}{C_{11}} - \frac{\rho(C_{12}^r)^2}{C_{11}^r} - \frac{(1-\rho)(C_{12}^m)^2}{C_{11}^m}, \tag{12}$$

$$Q_{66} = \frac{C_{66}^r C_{66}^m}{\rho C_{66}^m + (1-\rho)C_{66}^r}, \tag{13}$$

$$e_{11} = C_{11} \left[ \frac{\rho e_{11}^r}{C_{11}^r} + \frac{(1-\rho)e_{11}^m}{C_{11}^m} \right], \tag{14}$$

$$e_{12} = \rho e_{12}^r + (1-\rho)e_{12}^m + \frac{C_{12}e_{11}}{C_{11}} - \frac{\rho C_{12}^r e_{11}^r}{C_{11}^r} - \frac{(1-\rho)C_{12}^m e_{11}^m}{C_{11}^m}, \tag{15}$$

$$\epsilon_{11} = \frac{C}{B^2 + AC}, \tag{16}$$

where

$$A = \frac{\rho C_{55}^r}{(e_{15}^r)^2 + C_{55}^r \epsilon_{11}^r} + \frac{(1-\rho)C_{55}^m}{(e_{15}^m)^2 + C_{55}^m \epsilon_{11}^m}, \tag{17}$$

$$B = \frac{\rho e_{15}^r}{(e_{15}^r)^2 + C_{55}^r \epsilon_{11}^r} + \frac{(1-\rho)e_{15}^m}{(e_{15}^m)^2 + C_{55}^m \epsilon_{11}^m}, \tag{18}$$

$$C = \frac{\rho \epsilon_{11}^r}{(e_{15}^r)^2 + C_{55}^r \epsilon_{11}^r} + \frac{(1-\rho) \epsilon_{11}^m}{(e_{15}^m)^2 + C_{55}^m \epsilon_{11}^m}, \tag{19}$$

Superscripts *r* and *m* refer to the reinforced and matrix components of the composite, respectively.  $\rho$  is also the volume percent of the DWBNNTs in matrix.

### 4. Energy method

The total potential energy of the pipe is the sum of strain energy, *U* and the work *W* done by the applied load. The strain energy is

$$U_s = \int_V (\sigma_x \epsilon_x + \sigma_\theta \epsilon_\theta + \sigma_{x\theta} \gamma_{x\theta} - D_x E_x) dV. \tag{20}$$

Strain energy by combining Eq. (3) and Eq. (20) may be written as

$$U_s = \int_A \left( N_x \left( \frac{\partial u}{\partial x} + 0.5 \left( \frac{\partial w}{\partial x} \right)^2 \right) - M_x \frac{\partial^2 w}{\partial x^2} + N_\theta \left( \frac{\partial v}{R \partial \theta} + \frac{w}{R} + 0.5 \left( \frac{\partial w}{R \partial \theta} \right)^2 \right) - M_\theta \frac{\partial^2 w}{R^2 \partial \theta^2} + N_{x\theta} \left( \frac{\partial u}{R \partial \theta} + \frac{\partial v}{\partial x} + \frac{\partial w}{R \partial \theta} \frac{\partial w}{\partial x} \right) - 2M_{x\theta} \frac{\partial^2 w}{R \partial \theta \partial x} + G_x \frac{\partial \phi}{\partial x} \right) dA, \tag{21}$$

where the internal forces and moments may be expressed as

$$\begin{Bmatrix} N_x \\ N_\theta \\ N_{x\theta} \\ G_x \end{Bmatrix} = \int_{-\frac{h}{2}}^{\frac{h}{2}} \begin{Bmatrix} \sigma_x \\ \sigma_\theta \\ \tau_{x\theta} \\ D_x \end{Bmatrix} dz = \begin{bmatrix} A_{11} & A_{12} & 0 & P_{11} \\ A_{12} & A_{22} & 0 & P_{12} \\ 0 & 0 & A_{66} & 0 \\ P_{11} & P_{12} & 0 & Y_{11} \end{bmatrix} \begin{Bmatrix} \epsilon_x \\ \epsilon_\theta \\ \gamma_{x\theta} \\ E_x \end{Bmatrix}$$

$$-\begin{bmatrix} B_{11} & B_{12} & 0 & F_{11} \\ B_{12} & B_{22} & 0 & F_{12} \\ 0 & 0 & B_{66} & 0 \\ F_{11} & F_{12} & 0 & 0 \end{bmatrix} \begin{bmatrix} k_x \\ k_\theta \\ k_{x\theta} \\ E_x \end{bmatrix} = \begin{bmatrix} N_x^T \\ N_\theta^T \\ 0 \\ 0 \end{bmatrix}, \tag{22}$$

$$\begin{bmatrix} M_x \\ M_\theta \\ M_{x\theta} \\ Q_x \end{bmatrix} = \int_{-\frac{h}{2}}^{\frac{h}{2}} \begin{bmatrix} \sigma_x \\ \sigma_\theta \\ \tau_{x\theta} \\ D_x \end{bmatrix} z dz = \begin{bmatrix} B_{11} & B_{12} & 0 & F_{11} \\ B_{12} & B_{22} & 0 & F_{12} \\ 0 & 0 & B_{66} & 0 \\ F_{11} & F_{12} & 0 & H_{11} \end{bmatrix} \begin{bmatrix} \epsilon_x \\ \epsilon_\theta \\ \gamma_{x\theta} \\ E_x \end{bmatrix} \tag{23}$$

$$-\begin{bmatrix} S_{11} & S_{12} & 0 & J_{11} \\ S_{12} & S_{22} & 0 & J_{12} \\ 0 & 0 & S_{66} & 0 \\ J_{11} & J_{12} & 0 & 0 \end{bmatrix} \begin{bmatrix} k_x \\ k_\theta \\ k_{x\theta} \\ E_x \end{bmatrix} = \begin{bmatrix} M_x^T \\ M_\theta^T \\ 0 \\ 0 \end{bmatrix},$$

where

$$\begin{pmatrix} \{ A_{ij}, B_{ij}, S_{ij} \} \\ \{ P_{ij}, F_{ij}, J_{ij} \} \\ \{ Y_{ij}, H_{ij}, 0 \} \\ \{ N_n^T, M_n^T, 0 \} \end{pmatrix} = \int_{-\frac{h}{2}}^{\frac{h}{2}} \begin{pmatrix} \{1, z, z^2\} \\ \{1, z, z^2\} \\ \{1, z, 0\} \\ \{1, z, 0\} \end{pmatrix} \times \begin{pmatrix} \{C_{ij}\} \\ \{-e_{ij}\} \\ \{-\epsilon_{ij}\} \\ \{\alpha_n C_{ij}\} \end{pmatrix} dz \quad [i, j = 1, 2, \dots, 6] \quad [n = x, \theta]. \tag{24}$$

Substituting Eq. (3) into Eqs. (22) and (23) yields

$$N_x = \left( hC_{11} \left( \frac{\partial u}{\partial x} + 0.5 \left( \frac{\partial w}{\partial x} \right)^2 - \alpha_x \Delta T \right) + C_{12} \left( \frac{\partial v}{R \partial \theta} + \frac{w}{R} + 0.5 \left( \frac{\partial w}{R^2 \partial \theta} \right)^2 - \alpha_\theta \Delta T \right) + e_{11} \frac{\partial \phi}{\partial x} \right),$$

$$N_\theta = \left( hC_{12} \left( \frac{\partial u}{\partial x} + 0.5 \left( \frac{\partial w}{\partial x} \right)^2 - \alpha_x \Delta T \right) + C_{22} \left( \frac{\partial v}{R \partial \theta} + \frac{w}{R} + 0.5 \left( \frac{\partial w}{R^2 \partial \theta} \right)^2 - \alpha_\theta \Delta T \right) + e_{12} \frac{\partial \phi}{\partial x} \right), \tag{25}$$

$$N_{x\theta} = h \left( C_{66} \left( \frac{\partial u}{R \partial \theta} + \frac{\partial v}{\partial x} + \frac{\partial w}{R \partial \theta} \frac{\partial w}{\partial x} \right) \right),$$

$$G_x = e_{11} \left( \frac{\partial u}{\partial x} + 0.5 \left( \frac{\partial w}{\partial x} \right)^2 - \alpha_x \Delta T \right) + e_{12} \left( \frac{\partial v}{R \partial \theta} + \frac{w}{R} + 0.5 \left( \frac{\partial w}{R \partial \theta} \right)^2 - \alpha_\theta \Delta T \right) - \epsilon_{11} \frac{\partial \phi}{\partial x},$$

$$M_x = \frac{h^3}{12} \left( C_{11} \left( -z \frac{\partial^2 w}{\partial x^2} \right) + C_{12} \left( -z \frac{\partial^2 w}{R^2 \partial \theta^2} \right) \right),$$

$$M_\theta = \frac{h^3}{12} \left( C_{12} \left( -z \frac{\partial^2 w}{\partial x^2} \right) + C_{22} \left( -z \frac{\partial^2 w}{R^2 \partial \theta^2} \right) \right), \tag{26}$$

$$M_{x\theta} = \frac{h^3}{12} C_{66} \left( -2z \frac{\partial^2 w}{R \partial \theta \partial x} \right)$$

The work done by the nonhomogenous orthotropic elastic medium can be expressed as

(Kolahchi *et al.* 2015a, Mikhasev 2014)

$$W_{vs} = \int (F_e w) dA = \int \left( -k_w w + k_\xi (\cos^2 \alpha w_{,xx} + 2 \cos \alpha \sin \alpha w_{,yx} + \sin^2 \alpha w_{,yy}) + k_\eta (\sin^2 \alpha w_{,xx} - 2 \sin \theta \cos \alpha w_{,yx} + \cos^2 \alpha w_{,yy}) \right) w dA, \quad (27)$$

where angle  $\alpha$  describes the local  $\xi$  direction of orthotropic foundation with respect to the global  $x$ -axis of the plate and  $k_w$  is spring constant of elastic medium which may be written as

$$k_w = k_0 (1 - \beta \exp(-\chi x^2)), \quad (28)$$

where  $k_0 = 620 \times 10^{10}$  N/nm<sup>3</sup> and  $\chi > 1$ ,  $0 < \beta < 1$ . Applying Hamilton's principle and rearranging the governing equations in mechanical displacement directions ( $u, v$  and  $w$ ) as well as electric potential ( $\phi$ ), yield the following four coupled electro-thermo-mechanical equations

$$\begin{aligned} & (hC_{11}) \left( \frac{\partial^2 u}{\partial x^2} + \frac{\partial w}{\partial x} \frac{\partial^2 w}{\partial x^2} \right) + \frac{hC_{12}}{R} \left( \frac{\partial^2 v}{\partial x \partial \theta} + \frac{\partial w}{\partial x} + \frac{\partial w}{R \partial \theta} \frac{\partial^2 w}{\partial x \partial \theta} \right) \\ & + \frac{hC_{66}}{R} \left( \frac{\partial^2 u}{R \partial \theta^2} + \frac{\partial^2 v}{\partial x \partial \theta} + \frac{\partial w}{R \partial x} \frac{\partial^2 w}{\partial \theta^2} + \frac{\partial w}{\partial x} + \frac{\partial w}{R \partial \theta} \frac{\partial^2 w}{\partial x \partial \theta} \right) + h e_{11} \frac{\partial^2 \phi}{\partial x^2} = 0 \end{aligned} \quad (29)$$

$$\begin{aligned} & \frac{hC_{12}}{R} \left( \frac{\partial^2 u}{\partial x \partial \theta} + \frac{\partial w}{\partial x} \frac{\partial^2 w}{\partial x \partial \theta} \right) + \frac{hC_{22}}{R^2} \left( \frac{\partial^2 v}{\partial \theta^2} + \frac{\partial w}{\partial \theta} + \frac{\partial w}{R \partial \theta} \frac{\partial^2 w}{\partial \theta^2} \right) \\ & + hC_{66} \left( \frac{\partial^2 u}{R \partial x \partial \theta} + \frac{\partial^2 v}{\partial x^2} + \frac{\partial^2 w}{R \partial \theta \partial x} \frac{\partial w}{\partial x} + \frac{\partial w}{R \partial \theta} \frac{\partial^2 w}{\partial x^2} \right) + \frac{h e_{12}}{R} \frac{\partial^2 \phi}{\partial x \partial \theta} = 0, \end{aligned} \quad (30)$$

$$\begin{aligned} & \frac{h^3}{12} \left( -C_{11} \frac{\partial^4 w}{\partial x^4} - \frac{C_{12}}{R^2} \frac{\partial^4 w}{\partial x^2 \partial \theta^2} \right) + \frac{h^3 C_{66}}{3R^2} \left( -\frac{\partial^4 w}{\partial x^2 \partial \theta^2} \right) + \frac{h^3}{12R^2} \left( -C_{12} \frac{\partial^4 w}{\partial x^2 \partial \theta^2} - \frac{C_{66}}{R^2} \frac{\partial^4 w}{\partial \theta^4} \right) \\ & - \left( \frac{hC_{12}}{R} \right) \left( \frac{\partial u}{\partial x} + \frac{1}{2} \left( \frac{\partial w}{\partial x} \right)^2 \right) - \frac{hC_{22}}{R} \left( \frac{\partial v}{R \partial \theta} + \frac{w}{R} + \frac{1}{2R^2} \left( \frac{\partial w}{\partial \theta} \right)^2 \right) \\ & - \left( \frac{hC_{12} \alpha_x}{R^2} + \frac{hC_{22} \alpha_\theta}{R^2} \right) \frac{\partial^2 w}{\partial \theta^2} \Delta T - \left( N_x^M + hC_{11} \alpha_x + hC_{12} \alpha_\theta \right) \frac{\partial^2 w}{\partial x^2} \Delta T + \frac{\partial}{\partial x} \left( e_{11} \frac{\partial \phi}{\partial x} \frac{\partial w}{\partial x} \right) \\ & + \frac{\partial}{R^2 \partial \theta} \left( e_{12} \frac{\partial \phi}{\partial x} \frac{\partial w}{\partial \theta} \right) + \left( -k_0 (1 - \beta \exp(-\chi x^2)) w + k_\xi (\cos^2 \alpha w_{,xx} + 2 \cos \alpha \sin \alpha w_{,yx} + \sin^2 \alpha w_{,yy}) + k_\eta (\sin^2 \alpha w_{,xx} - 2 \sin \theta \cos \alpha w_{,yx} + \cos^2 \alpha w_{,yy}) \right) = 0, \end{aligned} \quad (31)$$

$$-\frac{\partial^2 \phi}{\partial x^2} + \left( \frac{e_{11}}{\epsilon_{11}} \right) \left( \frac{\partial^2 u}{\partial x^2} + \frac{\partial w}{\partial x} \frac{\partial^2 w}{\partial x^2} \right) + \frac{e_{12}}{R \epsilon_{11}} \left( \frac{\partial^2 v}{\partial x \partial \theta} + \frac{\partial w}{\partial x} + \frac{\partial w}{R \partial \theta} \frac{\partial^2 w}{\partial x \partial \theta} \right) = 0 \quad (32)$$

### 5. DQM

Here, DQM is used for solution. It is due to the fact that DQM is a powerful method which can be used to solve numerical problems in the analysis of structural and dynamical systems. In

addition, accuracy and convergence of the DQM is higher than finite element method (FEM), Due to the above striking merits of the DQM, in recent years the method has become increasingly popular in the numerical solution of problems in engineering and physical science. Hence, DQM is employed which in essence approximates the partial derivative of a function, with respect to a spatial variable at a given discrete point, as a weighted linear sum of the function values at all discrete points chosen in the solution domain of the spatial variable. Let  $F$  be a function representing  $u, v, w$  and  $\phi$  with respect to variables  $x$  and  $\theta$  in the following domain of ( $0 < x < L, 0 < \theta < 2\pi$ ) having  $N_x \times N_\theta$  grid points along these variables. The  $n^{\text{th}}$ -order partial derivative of  $F(x, \theta)$  with respect to  $x$ , the  $m^{\text{th}}$ -order partial derivative of  $F(x, \theta)$  with respect to  $\theta$  and the  $(n+m)^{\text{th}}$ -order partial derivative of  $F(x, \theta)$  with respect to both  $x$  and  $\theta$  may be expressed discretely at the point  $(x_i, \theta_j)$  as (Kolahchi *et al.* 2015b)

$$\frac{d^n f_x(x_i, \theta_j)}{dx^n} = \sum_{k=1}^{N_x} A_{ik}^{(n)} f(x_k, \theta_j) \quad n = 1, \dots, N_x - 1, \tag{33}$$

$$\frac{d^m f_y(x_i, \theta_j)}{d\theta^m} = \sum_{l=1}^{N_\theta} B_{jl}^{(m)} f(x_i, \theta_l) \quad m = 1, \dots, N_\theta - 1, \tag{34}$$

$$\frac{d^{n+m} f_{xy}(x_i, \theta_j)}{dx^n d\theta^m} = \sum_{k=1}^{N_x} \sum_{l=1}^{N_\theta} A_{ik}^{(n)} B_{jl}^{(m)} f(x_k, \theta_l). \tag{35}$$

A more superior choice for the positions of the grid points is Chebyshev polynomials as

$$x_i = \frac{L}{2} \left[ 1 - \cos\left(\frac{i-1}{N_x-1}\pi\right) \right] \quad i = 1, \dots, N_x, \tag{36}$$

$$\theta_i = \frac{2\pi}{2} \left[ 1 - \cos\left(\frac{i-1}{N_\theta-1}\pi\right) \right] \quad i = 1, \dots, N_\theta, \tag{37}$$

where  $A_{ik}^{(n)}$  and  $B_{jl}^{(m)}$  are the weighting coefficients associated with  $n^{\text{th}}$ -order partial derivative of  $F(x, \theta)$  with respect to  $x$  at the discrete point  $x_i$  and  $m^{\text{th}}$ -order derivative with respect to  $\theta$  at  $\theta_i$ , respectively which may be calculated as

$$A_{ij}^{(1)} = \begin{cases} \frac{M(x_i)}{(x_i - x_j)M(x_j)}, & \text{for } i \neq j, \quad i, j = 1, 2, \dots, N_x \\ -\sum_{\substack{j=1 \\ i \neq j}}^{N_x} A_{ij}^{(1)}, & \text{for } i = j, \quad i, j = 1, 2, \dots, N_x \end{cases} \tag{38}$$

$$B_{ij}^{(1)} = \begin{cases} \frac{P(\theta_i)}{(\theta_i - \theta_j)P(\theta_j)}, & \text{for } i \neq j, \quad i, j = 1, 2, \dots, N_\theta \\ -\sum_{\substack{j=1 \\ i \neq j}}^{N_\theta} B_{ij}^{(1)}, & \text{for } i = j, \quad i, j = 1, 2, \dots, N_\theta \end{cases} \tag{39}$$

where

$$M(x_i) = \prod_{\substack{j=1 \\ j \neq i}}^{N_x} (x_i - x_j), \tag{40}$$

$$P(\theta_i) = \prod_{\substack{j=1 \\ j \neq i}}^{N_\theta} (\theta_i - \theta_j). \tag{41}$$

For higher order derivatives we have

$$A_{ij}^{(n)} = n \left( A_{ii}^{(n-1)} A_{ij}^{(1)} - \frac{A_{ij}^{(n-1)}}{(x_i - x_j)} \right), \tag{42}$$

$$B_{ij}^{(m)} = m \left( B_{ii}^{(m-1)} B_{ij}^{(1)} - \frac{B_{ij}^{(m-1)}}{(\theta_i - \theta_j)} \right). \tag{43}$$

However, applying below dimensionless parameters

$$\begin{aligned} \gamma &= \frac{h}{L}, \quad \xi = \frac{x}{L}, \quad \beta = \frac{h}{R}, \quad \{\bar{u}, \bar{v}, \bar{w}\} = \frac{\{u, v, w\}}{h} \\ \bar{C}_{ij} &= \frac{C_{ij}}{C_{11}}, \quad K_w = \frac{hk_w}{C_{11}}, \quad K_g = \frac{k_g}{hC_{11}}, \\ \Phi &= \frac{\phi}{\Phi_0}, \quad \Phi_0 = h \sqrt{\frac{C_{11}}{\epsilon_{11}}}, \quad \bar{e}_{ij} = \frac{e_{ij}}{\sqrt{C_{11} \epsilon_{11}}}, \quad \bar{t} = \frac{t}{h \sqrt{\frac{\rho_f}{C_{s11}}}}, \end{aligned} \tag{44}$$

and using DQM, the governing equations may be written as

$$\begin{aligned} &(\gamma^2 \left( \sum_{k=1}^{N_x} A^{(2)}_{ik} \bar{w}(x_k, \theta_j) + \sum_{k=1}^{N_x} A^{(1)}_{ik} \bar{w}(x_k, \theta_j) \sum_{k=1}^{N_x} A^{(2)}_{ik} \bar{w}(x_k, \theta_j) \right) + \beta \gamma \bar{C}_{12} \left( \sum_{k=1}^{N_x} \sum_{p=1}^{N_\theta} A^{(1)}_{ik} B^{(1)}_{jp} \bar{w}(x_k, \theta_j) + \sum_{k=1}^{N_x} A^{(1)}_{ik} \bar{w}(x_k, \theta_j) \right. \\ &\left. \beta \sum_{p=1}^{N_\theta} B^{(1)}_{jp} \bar{w}(x_k, \theta_j) \sum_{k=1}^{N_x} \sum_{p=1}^{N_\theta} A^{(1)}_{ik} B^{(1)}_{jp} \bar{w}(x_k, \theta_j) \right) + \beta \bar{C}_{66} \left( \beta \sum_{p=1}^{N_\theta} B^{(2)}_{jp} \bar{u}(x_k, \theta_j) + \gamma \sum_{k=1}^{N_x} \sum_{p=1}^{N_\theta} A^{(1)}_{ik} B^{(1)}_{jp} \bar{v}(x_k, \theta_j) \right) \\ &+ \beta \sum_{k=1}^{N_x} A^{(1)}_{ik} \bar{w}(x_k, \theta_j) \sum_{p=1}^{N_\theta} B^{(2)}_{jp} \bar{w}(x_k, \theta_j) + \gamma \sum_{k=1}^{N_x} A^{(1)}_{ik} \bar{w}(x_k, \theta_j) + \beta \sum_{p=1}^{N_\theta} B^{(1)}_{jp} \bar{w}(x_k, \theta_j) \sum_{k=1}^{N_x} \sum_{p=1}^{N_\theta} A^{(1)}_{ik} B^{(1)}_{jp} \bar{v}(x_k, \theta_j) \Big) \\ &+ \gamma^2 \bar{e}_{11} \sum_{k=1}^{N_x} A^{(2)}_{ik} \Phi(x_k, \theta_j) = 0, \end{aligned} \tag{45}$$

$$\begin{aligned} &\beta \bar{C}_{12} \left( \gamma \sum_{k=1}^{N_x} \sum_{p=1}^{N_\theta} A^{(1)}_{ik} B^{(1)}_{jp} \bar{u}(x_k, \theta_j) + \gamma^2 \sum_{k=1}^{N_x} A^{(1)}_{ik} \bar{w}(x_k, \theta_j) \sum_{k=1}^{N_x} \sum_{p=1}^{N_\theta} A^{(1)}_{ik} B^{(1)}_{jp} \bar{w}(x_k, \theta_j) \right) + \beta^2 \bar{C}_{22} \left( \sum_{p=1}^{N_\theta} B^{(2)}_{jp} \bar{v}(x_k, \theta_j) \right. \\ &+ \sum_{p=1}^{N_\theta} B^{(1)}_{jp} \bar{w}(x_k, \theta_j) + \beta \sum_{p=1}^{N_\theta} B^{(1)}_{jp} \bar{w}(x_k, \theta_j) \sum_{p=1}^{N_\theta} B^{(2)}_{jp} \bar{w}(x_k, \theta_j) \Big) + \gamma \bar{C}_{66} \left( \beta \sum_{k=1}^{N_x} \sum_{p=1}^{N_\theta} A^{(1)}_{ik} B^{(1)}_{jp} \bar{u}(x_k, \theta_j) + \gamma \sum_{k=1}^{N_x} A^{(2)}_{ik} \bar{w}(x_k, \theta_j) \right. \\ &+ \beta \gamma \sum_{k=1}^{N_x} \sum_{p=1}^{N_\theta} A^{(1)}_{ik} B^{(1)}_{jp} \bar{w}(x_k, \theta_j) \sum_{k=1}^{N_x} A^{(1)}_{ik} \bar{w}(x_k, \theta_j) + \beta \gamma \sum_{p=1}^{N_\theta} B^{(1)}_{jp} \bar{w}(x_k, \theta_j) \sum_{k=1}^{N_x} A^{(2)}_{ik} \bar{w}(x_k, \theta_j) \Big) \\ &+ \gamma_s \bar{C}_{s66} \left( \beta_s \sum_{k=1}^{N_x} \sum_{p=1}^{N_\theta} A^{(1)}_{ik} B^{(1)}_{jp} \bar{u}(x_k, \theta_j) + \sum_{k=1}^{N_x} A^{(2)}_{ik} \bar{v}(x_k, \theta_j) + \beta \bar{e}_{12} \sum_{k=1}^{N_x} \sum_{p=1}^{N_\theta} A^{(1)}_{ik} B^{(1)}_{jp} \Phi(x_k, \theta_j) \right) = 0, \end{aligned} \tag{46}$$

$$\begin{aligned}
 & \frac{\gamma^2}{12} \left( -\gamma^2 \sum_{k=1}^{N_x} A^{(4)}_{ik} \bar{w}(x_k, \theta_j) - \bar{C}_{12} \beta^2 \sum_{k=1}^{N_x} \sum_{p=1}^{N_\theta} A^{(2)}_{ik} B^{(2)}_{jp} \bar{w}(x_k, \theta_j) \right) - \frac{\gamma^2 \beta^2 \bar{C}_{66}}{3} \left( \sum_{k=1}^{N_x} \sum_{p=1}^{N_\theta} A^{(2)}_{ik} B^{(2)}_{jp} \bar{w}(x_k, \theta_j) \right) \\
 & + \frac{1}{12} \left( -\beta^4 \bar{C}_{66} \sum_{k=1}^{N_x} \sum_{p=1}^{N_\theta} A^{(2)}_{ik} B^{(2)}_{jp} \bar{w}(x_k, \theta_j) - \gamma^2 \beta^2 \bar{C}_{12} \sum_{p=1}^{N_\theta} B^{(4)}_{jp} \bar{w}(x_k, \theta_j) \right) - \gamma \beta \bar{C}_{12} \left( \sum_{k=1}^{N_x} A^{(1)}_{ik} \bar{u}(x_k, \theta_j) + \frac{\gamma}{2} \sum_{k=1}^{N_x} A^{(1)}_{ik} \bar{w}(x_k, \theta_j) \sum_{k=1}^{N_x} A^{(1)}_{ik} \bar{w}(x_k, \theta_j) \right) \\
 & - \beta \bar{C}_{22} \left( \beta \sum_{p=1}^{N_\theta} B^{(1)}_{jp} \bar{v}(x_k, \theta_j) + \beta \bar{w}(x_k, \theta_j) + \frac{\beta^2}{2} \sum_{p=1}^{N_\theta} B^{(1)}_{jp} \bar{w}(x_k, \theta_j) \sum_{p=1}^{N_\theta} B^{(1)}_{jp} \bar{w}(x_k, \theta_j) \right) - \left( \beta^2 \alpha_x \bar{C}_{12} + \beta^2 \bar{C}_{22} \alpha_\theta \right) \Delta T \sum_{p=1}^{N_\theta} B^{(2)}_{jp} \bar{w}(x_k, \theta_j) \\
 & - \left( \gamma^2 \alpha_x + \gamma^2 \bar{C}_{12} \alpha_\theta \right) \sum_{k=1}^{N_x} A^{(2)}_{ik} \bar{w}(x_k, \theta_j) \Delta T - k_0 (1 - \beta \exp(-\chi x_k^2)) \bar{w}(x_k, \theta_j) \tag{47}
 \end{aligned}$$

$$\begin{aligned}
 & + k_\xi \left( \cos^2 \alpha \sum_{k=1}^{N_x} A^{(2)}_{ik} \bar{w}(x_k, \theta_j) + 2 \cos \alpha \sin \alpha \left( \sum_{k=1}^{N_x} \sum_{p=1}^{N_\theta} A^{(2)}_{ik} B^{(2)}_{jp} \bar{w}(x_k, \theta_p) \right) + \sin^2 \alpha \sum_{p=1}^{N_\theta} B^{(2)}_{jp} \bar{w}(x_p, \theta_j) \right) \\
 & + k_\eta \left( \sin^2 \alpha \sum_{k=1}^{N_x} A^{(2)}_{ik} \bar{w}(x_k, \theta_j) - 2 \sin \alpha \cos \alpha \left( \sum_{k=1}^{N_x} \sum_{p=1}^{N_\theta} A^{(2)}_{ik} B^{(2)}_{jp} \bar{w}(x_k, \theta_p) \right) + \cos^2 \alpha \sum_{p=1}^{N_\theta} B^{(2)}_{jp} \bar{w}(x_p, \theta_j) \right) \\
 & + \sum_{k=1}^{N_x} A^{(1)}_{ik} \left( e_{11} \sum_{k=1}^{N_x} A^{(1)}_{kl} \Phi(x_k, \theta_j) \sum_{k=1}^{N_x} A^{(1)}_{jm} \bar{w}(x_j, \theta_b) \right) + \beta^2 \sum_{k=1}^{N_\theta} B^{(1)}_{ik} \left( e_{12} \sum_{k=1}^{N_\theta} B^{(1)}_{kl} \Phi(x_k, \theta_j) \sum_{k=1}^{N_\theta} A^{(1)}_{jm} \bar{w}(x_j, \theta_b) \right) = \ddot{\bar{w}}(x_j, \theta_j), \\
 & - \sum_{k=1}^{N_x} A^{(2)}_{ik} \Phi(x_k, \theta_j) + \bar{e}_{11} \left( \sum_{k=1}^{N_x} A^{(2)}_{ik} \bar{u}(x_k, \theta_j) + \gamma \sum_{k=1}^{N_x} A^{(1)}_{ik} \bar{w}(x_k, \theta_j) \sum_{k=1}^{N_x} A^{(2)}_{ik} \bar{w}(x_k, \theta_j) \right) \\
 & + \frac{\beta \bar{e}_{12}}{\gamma} \left( \sum_{k=1}^{N_x} \sum_{p=1}^{N_\theta} A^{(1)}_{ik} B^{(1)}_{jp} \bar{v}(x_k, \theta_j) + \sum_{k=1}^{N_x} A^{(1)}_{ik} \bar{w}(x_k, \theta_j) + \frac{\beta}{\gamma} \sum_{p=1}^{N_\theta} B^{(1)}_{jp} \bar{w}(x_k, \theta_j) \sum_{k=1}^{N_x} \sum_{p=1}^{N_\theta} A^{(1)}_{ik} B^{(1)}_{jp} \bar{v}(x_k, \theta_j) \right) = 0 \tag{48}
 \end{aligned}$$

According to DQM, mechanical and electrical boundary conditions may be written as

$$\begin{cases} w_{i1} = v_{i1} = u_{i1} = \phi_{i1} = 0, & \sum_{j=1}^{N_\theta} A_{2j} w_{ji} = 0 \\ w_{N_x i} = v_{N_x i} = u_{N_x i} = \phi_{N_x i} = 0, & \sum_{j=1}^{N_\theta} A_{(N_x-1)j} w_{ji} = 0 \end{cases} \quad \text{for } i=1 \dots N_\theta \tag{49}$$

Applying these boundary conditions into the Eqs. (45)-(48) yields the following coupled governing equations in matrix form as

$$\left( \left[ \underbrace{K_L + K_{NL}}_K \right] + N_x^{M^2} [K_G] \right) \begin{Bmatrix} \{d_b\} \\ \{d_d\} \end{Bmatrix} = 0, \tag{50}$$

where  $K_L$ ,  $K_{NL}$  and  $K_G$  are linear stiffness matrix, nonlinear stiffness matrix and geometric matrix, respectively. Also,  $d_b$  and  $d_d$  represent boundary and domain points expressed as

$$\begin{aligned}
 \{d_b\} &= \{ \bar{u}_{i1}, \bar{v}_{i1}, \bar{w}_{i1}, \bar{w}_{i2}, \Phi_{i1}, \bar{u}_{iN_\theta}, \bar{v}_{iN_\theta}, \bar{w}_{iN_\theta}, \bar{w}_{i(N_\theta-1)}, \Phi_{iN_\theta} \} \quad i=1, \dots, N_x \\
 \{d_d\} &= \{ \bar{u}_{ij}, \bar{v}_{ij}, \bar{w}_{i(j+1)}, \Phi_{ij} \} \quad i=1, \dots, N_x, \quad j=2, \dots, N_x-1 \end{aligned} \tag{51}$$

Finally, based on an iterative method and eigenvalue problem, the buckling load of structure may be obtained.

### 6. Numerical result

Mechanical, electrical and thermal characteristics of PVDF as matrix and DWBNNTs as

reinforcer are assumed as (Mosallaie Barzoki *et al.* 2013)

$$C_{11}^m = 10.64 \text{ GPa} \quad C_{23}^m = 3.98 \text{ GPa} \quad E_p = 1.8 \text{ TPa} \quad \nu_p = 0.34$$

$$C_{22}^m = 23.6 \text{ GPa} \quad \alpha_{11}^m = \alpha_{22}^m = \alpha_{33}^m = 7.1e-5 \frac{1}{^\circ\text{C}}$$

$$C_{44}^m = 6.43 \text{ GPa} \quad \alpha_{22}^p = 0.6e-6 \frac{1}{^\circ\text{C}} \quad \alpha_{33}^p = 1.2e-6 \frac{1}{^\circ\text{C}}$$

$$C_{12}^m = 1.92 \text{ GPa} \quad e_{11}^p = 0.95 \text{ C/m}^2$$

$$C_{13}^m = 2.19 \text{ GPa} \quad e_{11}^m = -0.13 \text{ C/m}^2 \quad e_{12}^m = -0.145 \text{ C/m}^2 \quad e_{31}^m = -0.135 \text{ C/m}^2$$

In order to obtain the buckling load for considered pipe embedded in the elastic foundation, DQM was used in conjunction with a program being written in MATLAB, where the effect of smartness, volume percent of DWBNNTs, orientation angle of DWBNNTs and elastic medium were investigated.

### 6.1 Validation

To demonstrate the validity of this work, present results are compared with those reported by (Mosallaie Barzoki *et al.* 2013), For this purpose, ignoring the orthotropic nonhomogeneous Pasternak medium, the non-dimensional buckling load of pipe with clamped supported boundary condition is shown in Fig. 1. As can be seen, present results are in good agreement with those reported by (Mosallaie Barzoki *et al.* 2013), indicating validation of present work.

### 6.2 Convergence of DQM

The effect of the grid point number in DQM on the buckling of the pipe is demonstrated in Fig.

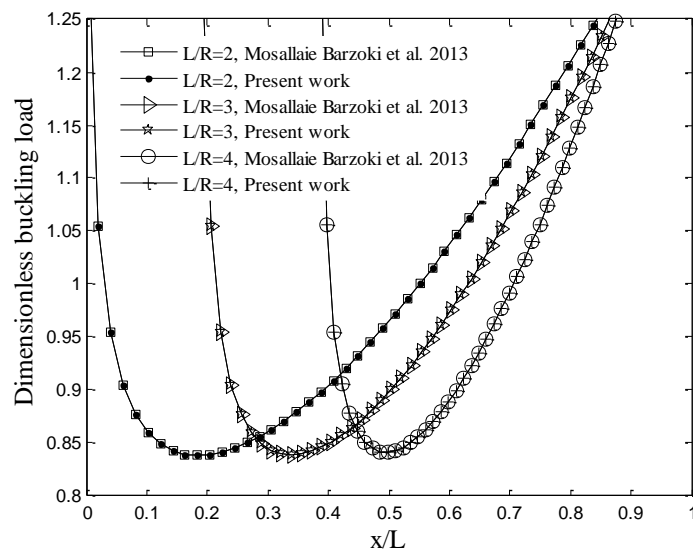


Fig. 1 validation of present work with (Mosallaie Barzoki *et al.* 2013)

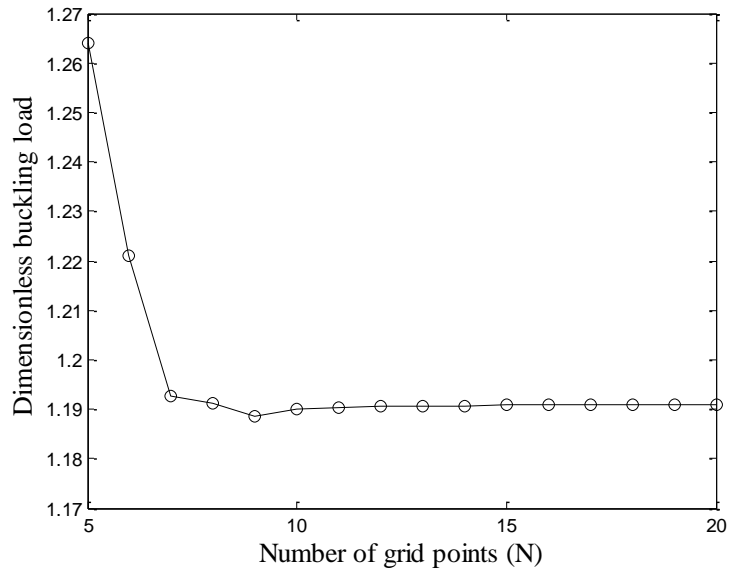


Fig. 2 Convergence and accuracy of DQM

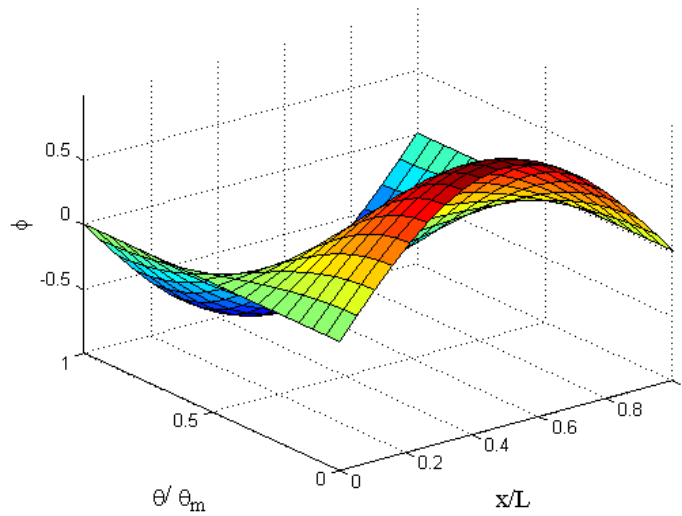


Fig. 3 Electric potential distribution for first mode

2. As can be seen, fast rate of convergence of the method are quite evident and it is found that 15 DQ grid points can yield accurate results.

### 6.3 Smartness effect

Figs. 3-5 illustrate the smartness effect due to pipe piezoelectricity at different modes. In this figures, the electric potential is plotted against the dimensionless length ( $x/L$ ) and dimensionless angle ( $\theta/\theta_m$ ) where  $\theta_m=2\pi$ . It is worth to mention that the electric potential has distribution while

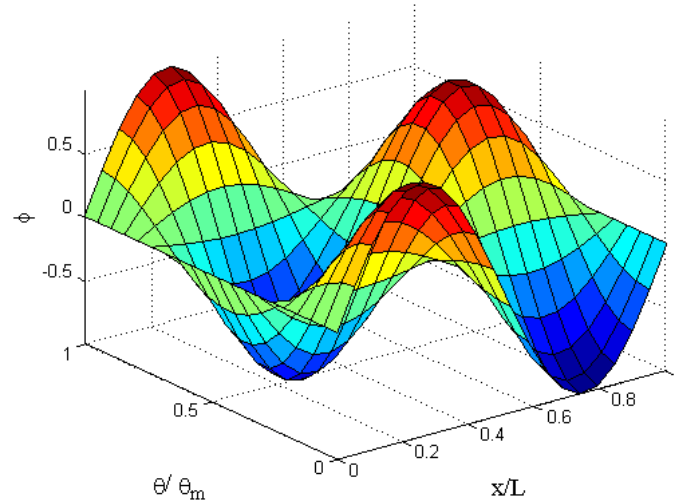


Fig. 4 Electric potential distribution for second mode

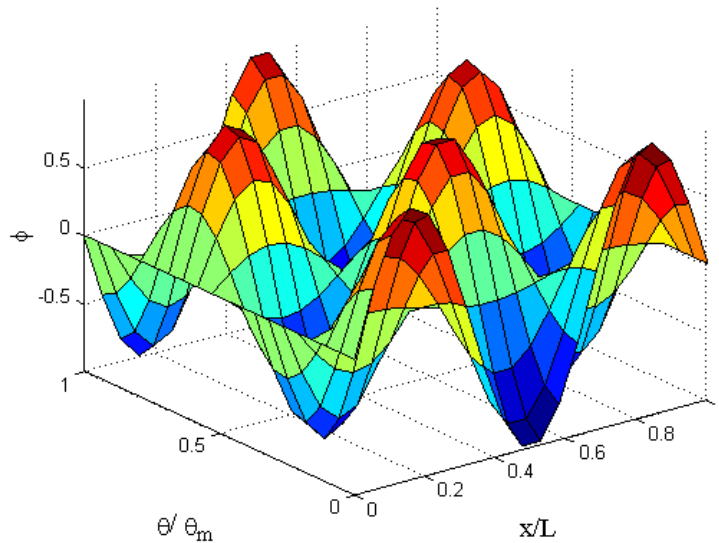


Fig. 5 Electric potential distribution for third mode

the electrical boundary condition is assumed zero in Eq. (49), This result shows the specific characteristic of piezoelectric material which can use from these materials in sensors and actuators. Furthermore, the electrical boundary conditions at the first and last ends of pipe are satisfied. Noted that according to Eq. (49), the electric potential is zero in both ends of the pipe (i.e., axial polarization).

#### 6.4 Nanotechnology effect

Figs. 6 and 7 demonstrate the nanotechnology effect in buckling of pipes. For this end, the pipe

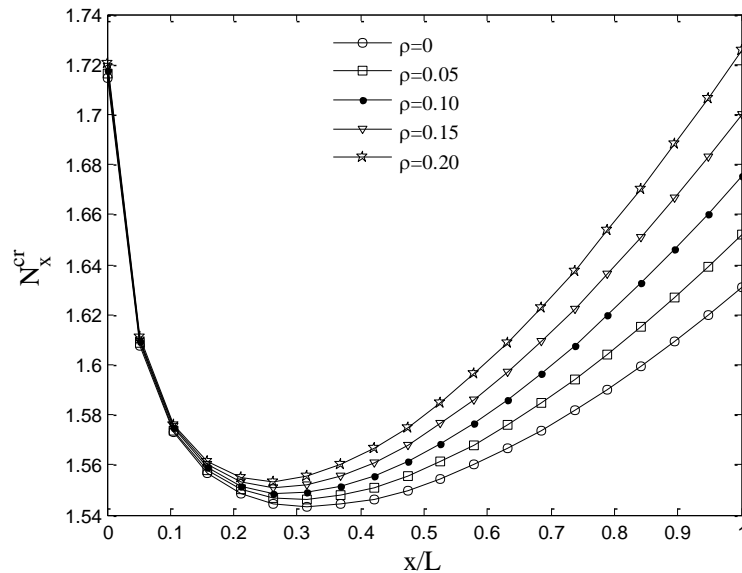


Fig. 6 Volume percent of DWBNNTs effects on the buckling load of pipe

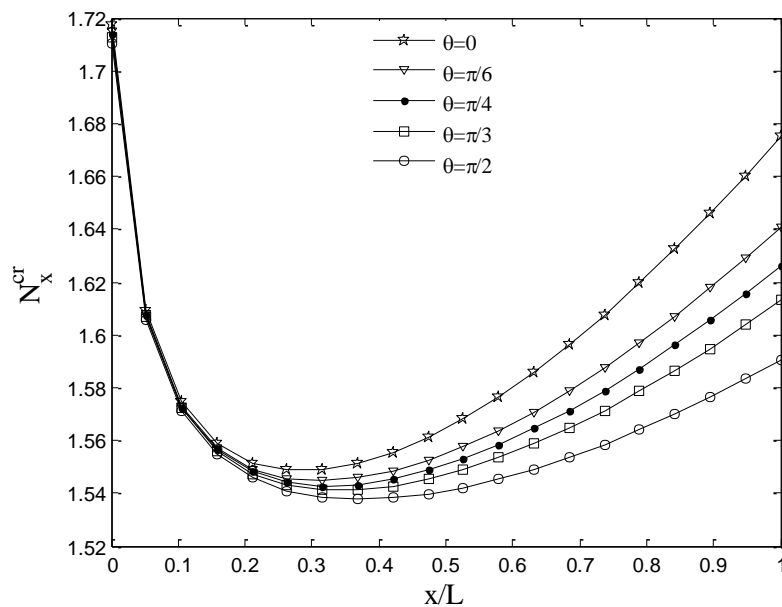


Fig. 7 Orientation angle of DWBNNTs effects on the buckling load of pipe

is reinforced with DWBNNTs and the effect of volume percent and orientation angle of them in pipe on the buckling load are shown. From Fig. 6, it can be found that with increasing volume percent of DWBNNTs in pipe, the buckling load increases. It is due to the fact that with increasing volume percent of DWBNNTs in pipe, the stiffness of structure increases. As can be seen from Fig. 7, with increasing the orientation angle of DWBNNTs, the buckling load decreases. Hence,

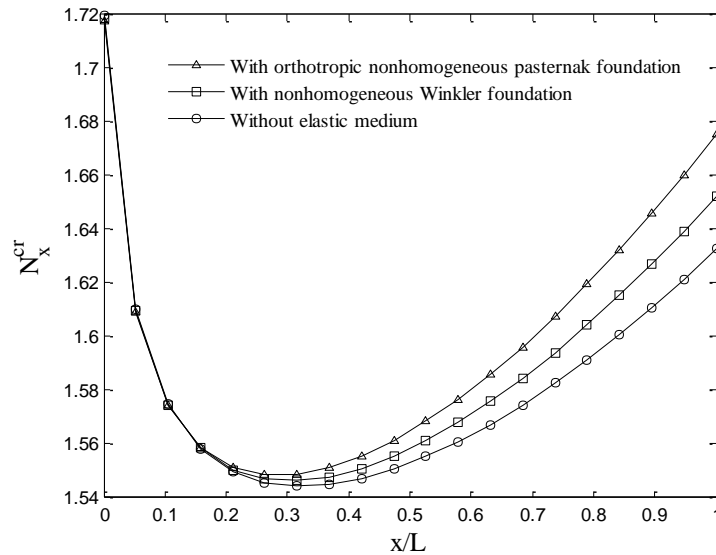


Fig. 8 Elastic medium effects on the buckling load of pipe

maximum and minimum buckling load are related to  $\theta=0$  and  $\theta=\pi/2$ , respectively. It is due to the fact that in  $\theta=0$ , the polarization of pipe and DWBNNTs are in a one direction and consequently, the stiffness of structure is maximum. Hence, the DWBNNT volume fraction and orientation angle in pipe are effective controlling parameters for buckling of the pipes.

### 6.5 Orthotropic nonhomogeneous elastic medium effect

Fig. 8 illustrate the influence of elastic medium, including Winkler and Pasternak modules, on the buckling load, along the length of the pipe. Obviously, the elastic medium type has a significant effect on buckling of the pipe, since the buckling load of the system in the case of without elastic medium are lower than other cases. It can be concluded that the buckling load for orthotropic nonhomogeneous Pasternak model is higher than nonhomogeneous Winkler one. The above results are reasonable, since the orthotropic nonhomogeneous Pasternak medium considers not only the normal stresses (i.e., nonhomogeneous Winkler foundation) but also the transverse shear deformation and continuity among the spring elements.

## 7. Conclusions

Pipes have vast applications in many engineering fields such as chemical, mechanical aerospace, civil, naval, and nuclear industries. However, in this paper, the nanotechnology and smartness effects were studied on the buckling behaviors of embedded pipes. The surrounding elastic medium is simulated with a very novel model namely as orthotropic nonhomogeneous Pasternak medium. Using DQM, the derived governing equations were discretized and solved to obtain the buckling load with clamped-clamped boundary condition. Numerical results indicate that the electric potential has distribution while the electrical boundary condition is assumed zero.

This result shows the specific characteristic of piezoelectric material which can use from these materials in sensors and actuators. Furthermore, it can be found that with increasing volume percent of DWBNNTs in pipe, the buckling load increases. Also, maximum and minimum buckling load are related to  $\theta=0$  and  $\theta=\pi/2$ , respectively. Obviously, the elastic medium type has a significant effect on the buckling load of the pipe since in the case of neglecting elastic foundation, the buckling load decreases especially at the end of the pipe. It is hoped that the obtained results might be useful for the design and improvement of smart devices applying nanotechnology.

## References

- Agarwal, B.L. and Sobel, L.H. (1977), "Weight comparisons of optimized stiffened, un stiffened, and sandwich cylindrical shells", *AIAA J.*, **14**, 1000-1008.
- Brockmann, T.H. (2009), *Theory of adaptive fiber composites from piezoelectric material behavior to dynamics of rotating structures*, Springer, USA.
- Brush, D.O. and Almroth, B.O. (1975), *Buckling of bars, plates and shells*, McGraw-Hill, New York.
- Ghorbanpour Arani, A., Golabi, S., Loghman, A. and Daneshi, H. (2007), "Investigating elastic stability of cylindrical shell with an elastic core under axial compression by energy method", *J. Mech. Sci. Tech.*, **21**, 693-698.
- Ghorbanpour Arani, A., Kolahchi, R., Mosallaie Barzoki, A.A. and Loghman, A. (2011a), "Electro-thermomechanical behaviors of FGPM spheres using analytical method and ANSYS software", *J. Appl. Math. Model.*, **36**, 139-157.
- Ghorbanpour Arani, A., Kolahchi, R. and Mosallaie Barzoki, A.A. (2011b), "Effect of material inhomogeneity on electro-thermo-mechanical behaviors of functionally graded piezoelectric rotating cylinder", *J. Appl. Math. Model.*, **35**, 2771-2789.
- Ghorbanpour Arani, Abdollahian, M. and Kolahchi, R. (2015a), "Nonlinear vibration of embedded smart composite microtube conveying fluid based on modified couple stress theory", *Polym. Compos.*, **36**, 1314-1324.
- Ghorbanpour Arani, A., Kolahchi, R. and Zarei, M.Sh. (2015b), "Visco-surface-nonlocal piezoelectricity effects on nonlinear dynamic stability of graphene sheets integrated with ZnO sensors and actuators using refined zigzag theory", *Compos. Struct.*, **132**, 506-526.
- Hutchinson, J.W. and He, M.Y. (2000), "Buckling of cylindrical sandwich shells with metal foam cores", *Int. J. Solid. Struct.*, **37**, 6777-6794.
- Junger, M.C. and Mass, C. (1952), "Vibration of elastic shells in a fluid medium and the associated radiation of sound", *J. Appl. Mech.*, **74**, 439-445.
- Karam, G.N. and Gibson, L.J. (1995), "Elastic buckling of cylindrical shells with elastic cores I. analysis", *Int. J. Solid. Struct.*, **32**, 1259-1283.
- Khayat, M., Poorveis, D., Moradi, Sh. and Hemmati, M. (2016), "Buckling of thick deep laminated composite shell of revolution under follower forces", *Struct. Eng. Mech.*, **58**, 59-91.
- Kotsilkova, R. (2007), *Thermoset Nanocomposites for Engineering Applications*, Smithers Rapra Technology, USA.
- Kolahchi, R., Moniri Bidgoli, A.M. and Heydari M.M. (2015a), "Size-dependent bending analysis of FGM nano-sinusoidal plates resting on orthotropic elastic medium", *Struct. Eng. Mech.*, **55**, 1001-1014.
- Kolahchi, R., Rabani Bidgoli, M., Beygipoor, Gh. and Fakhari, M.H. (2015b), "A nonlocal nonlinear analysis for buckling in embedded FG-SWCNT-reinforced microplates subjected to magnetic field", *J. Mech. Sci. Tech.*, **29**, 3669-3677.
- Kolahchi, R. and Moniribidgoli, A.M. (2016), "Size-dependent sinusoidal beam model for dynamic instability of single-walled carbon nanotubes", *Appl. Math. Mech.*, **37**, 265-274.
- MerhariHybrid, L. (2002), *Nanocomposites for Nanotechnology*, Springer Science, New York.

- Mikhasev, G. (2014), "On localized modes of free vibrations of single-walled carbon nanotubes embedded in nonhomogeneous elastic medium", *ZAMM Z. Angew. Math. Mech.*, **94**, 130-141.
- Mohammadi, H., Mahzoon, M., Mohammadi, M. and Mohammadi, M. (2014), "Postbuckling instability of nonlinear nanobeam with geometric imperfection embedded in elastic foundation", *Nonlin. Dyn.*, **76**, 2005-2016.
- Mosallaie Barzoki, A.A., Ghorbanpour Arani, A., Kolahchi, R., Mozdianfard, M.R. and Loghman, A. (2013), "Nonlinear buckling response of embedded piezoelectric cylindrical shell reinforced with BNNT under electro-thermo-mechanical loadings using HDQM", *Compos. Part B*, **44**, 722-727.
- Nasihatgozar, M., Daghigh, V., Eskandari, M., Nikbin, K., Simoneaud, A. (2016), "Buckling analysis of piezoelectric cylindrical composite panels reinforced with carbon nanotubes", *Int. J. Mech. Sci.*, **107**, 69-79.
- Nguyen-Van, H., Mai-Duy, N., Karunasena, W. and Tran-Cong, T. (2011), "Buckling and vibration analysis of laminated composite plate/shell structures via a smoothed quadrilateral flat shell element with in-plane rotations", *Compos. Struct.*, **89**, 612-625.
- Rabani Bidgoli, M., Karimi, M.S. Ghorbanpour Arani, A. (2015), "Viscous fluid induced vibration and instability of FG-CNT-reinforced cylindrical shells integrated with piezoelectric layers", *Steel Compos. Struct.*, **19**, 713-733.
- Rahmani, O., Khalili, S.M.R. and Malekzadeh, K. (2010), "Free vibration response of composite sandwich cylindrical shell with flexible core", *Compos. Struct.*, **92**, 1269-1281.
- Salehi-Khojin, A. and Jalili, N. (2008), "Buckling of boron nitride nanotube reinforced piezoelectric polymeric composites subject to combined electro-thermo-mechanical loadings", *Compos. Sci. Technol.*, **68**, 1489-1501.
- Schwartz, M. (2009), *SMART MATERIALS* by John Wiley and Sons, A Wiley-Interscience Publication Inc., New York.
- Sun, J., Xu, X., Lim, C.W., Zhou, Zh. and Xiao, S. (2016), "Accurate thermo-electro-mechanical buckling of shear deformable piezoelectric fiber-reinforced composite cylindrical shells", *Compos. Struct.*, **141**, 221-231.
- Tan, P. and Tong, L. (2001), "Micro-electromechanics models for piezoelectric-fiber-reinforced composite materials", *Compos. Sci. Technol.*, **61**, 759-769.
- Vang, J. (2006), *The Mechanics of Piezoelectric Structures*, World Scientific Publishing Co, USA.
- Yu, V. (2009), *Christopher, T., Bowen, R: Electromechanical Properties in Composites Based on Ferroelectrics*, Springer-Verlag, London.
- Ye, L., Lun, G. and Ong, L.S. (2011), "Buckling of a thin-walled cylindrical shell with foam core under axial compression", *Thin Wall. Struct.*, **49**, 106-111.